Silva AC, Zhang W, Williams DS & Koretsky AP.Estimation of water extraction fractions in rat brain using magnetic resonance measurement of perfusion with arterial spin labeling. Ma...

ARTICLE *in* MAGNETIC RESONANCE IN MEDICINE · JANUARY 1997

Impact Factor: 3.57 · DOI: 10.1002/mrm.1910370110 · Source: PubMed

Estimation of Water Extraction Fractions in Rat Brain Using Magnetic Resonance Measurement of Perfusion with Arterial Spin Labeling

Afonso C. Silva, Weiguo Zhang, Donald S. Williams, Alan P. Koretsky

The model used for calculating perfusion by MRI techniques that use endogenous water as a tracer assumes that arterial water is a freely diffusible tracer. Evidence shows that this assumption is not valid in the brain at high blood flow rates, at which movement of water into and out of the microvasculature becomes limited by diffusion across the blood-brain barrier. In this work, the arterial spin-labeling technique is used to show that fraction of arterial water that is dependent on blood flow rate remains in the vasculature and does not exchange with brain tissue water. By using perfusion measurements without and with magnetization transfer (MT) effects, one can distinguish arterial label that exchanges into tissue because blood has much smaller MT than brain tissue. Using this technique, the extraction fraction for water is measured in the rat brain at various cerebral blood flow rates. At high flow rates (~5 ml/g/min), the extraction fraction for water is found to be about 45% in rat brain. Disruption of the blood-brain barrier with D-mannitol caused an increase in the extraction fraction for water. It was possible to form an image related to the extraction fraction for water. The ability to estimate the amount of vascular water exchanging with tissue water by MRI may represent a noninvasive approach to detect the integrity of the blood-brain barrier.

Key words: Cerebral blood flow; endogenous perfusion tracers; magnetization transfer; blood-brain barrier.

INTRODUCTION

Endogenous water can serve as a tracer for MRI of perfusion according to a number of different approaches (1–17). Continuous arterial spin labeling was originally proposed by Detre *et al.* using saturation of arterial water spins (1) and by Williams *et al.* using inversion of the arterial spins (2). This technique has been applied successfully to quantitate tissue perfusion in the brain (1–8), kidney (9), and isolated perfused heart (10). Recently, continuous arterial spin labeling has been extended to human applications, particularly for measuring perfusion in the kidneys (11) and brain (12). A different approach is to pulse label the arterial water spins by application of a slab-selective 180° RF pulse, for example, to invert the arterial spins. The EPISTAR technique by Edelman *et al.* (13) represents a variation of this pulsed labeling method.

In all of these techniques, the arterial spins are labeled magnetically by the use of RF excitation selective at a plane proximal to the organ of interest. The inflowing labeled spins exchange with tissue water, causing a net change in tissue magnetization. This change can be used to calculate the perfusion rate, according to a modification of the Bloch equations to include the effects of blood flow for the particular labeling performed (1).

Arterial water also can be used as an endogenous tracer by labeling the tissue water with respect to blood water rather than labeling the blood water with respect to tissue water. Recently, selective T_1 measurements have been compared to nonselective T_1 measurements to estimate perfusion (14–17). The modified Bloch equations for longitudinal tissue water magnetization predict that the apparent relaxation of tissue water, T_{1app}, in the presence of blood flow is given by $1/T_{1app} = 1/T_1 + f/\lambda$, if a slice in the organ of interest is selectively inverted with respect to inflowing arterial blood (2, 3, 14–17). Changes in T_{1app} have been verified to be related to changes in perfusion in the heart (10), and T_1 weighting has been useful for monitoring task activation in the human brain (14). If a broad region is inverted nonselectively, so that inflowing blood and tissue are inverted, then the T_1 measured is independent of blood flow, assuming that blood and tissue water have similar T_1. The determination of selective (tissue only) and nonselective (tissue and inflowing blood) relaxation times allows for quantitation of perfusion. This method was reported independently by Kwong *et al.* (14, 15), Kim (16), and Schwarzbauer *et al.* (17).

The model used by all of the above techniques assumes that labeled arterial water is a freely diffusible tracer. Although this assumption seems to be valid in organs such as the heart over a large range of blood flow rates, evidence shows that it is not valid in the brain (18–22). In the adult rhesus monkey brain, for example, the extraction fraction for water is about 90% at normal cerebral blood flow (CBF) (~0.5 ml/g/min) and decreases progressively with increasing CBF (18, 20, 21). It is believed that the blood-brain barrier plays a role in limiting exchange between vascular water and tissue water.

MRM 35:58–68 (1997)

From the Pittsburgh NMR Center for Biomedical Research (A.C.S., W.Z., D.S.W. A.P.K.), the Department of Biological Sciences (A.P.K.), and the Biomedical Engineering Program (A.C.S.), Carnegie Mellon University, Pittsburgh, Pennsylvania.

Address correspondence to: Alan P. Koretsky, Ph.D., Department of Biological Sciences, Carnegie Mellon University, 4400 Fifth Avenue, Pittsburgh, PA 15213.

Present address (W.Z.): Radiologic Imaging Laboratory, Toshiba America MRI, Inc., 400 Grandview Drive, South San Francisco, CA 94080.

Received February 14, 1996; revised June 27, 1996; accepted July 1, 1996.

This work was supported by an NIH Research Resource Award (RR-03631) to the Pittsburgh NMR Center for Biomedical Research, an NIH Research Career Development Award (HL-02847-02) to A.P.K., and a Brazilian Scientific and Technological Development Council (CNPq-201088/92-4) fellowship to A.C.S. Financial support for the establishment of the Pittsburgh NMR Center for Biomedical Research was provided by the Richard King Mellon Foundation, the Lucille Markey Charitable Trust, the Ralph M. Parsons Foundation, and the Ben Franklin Partnership Program of the Commonwealth of Pennsylvania.

0740-3194/97 $3.00

In this work, NMR measurements of perfusion using continuous arterial spin labeling are performed to *non-invasively* measure the extraction fraction for water in the rat brain at different CBF values. The key to making an estimate of the extraction is to compare perfusion values measured using arterial spin labeling with and without saturation of macromolecular spins to give rise to a magnetization transfer effect. Because blood and tissue have very different magnetization transfer effects, it is possible to determine whether labeled spins have diffused into tissue, allowing an estimate of the extraction fraction. The extraction fraction for water is incorporated directly into the Bloch equations, and quantitation of perfusion according to this modified model is explained. It is shown that the extraction fraction decreases with increasing CBF. To show that the value of the extraction fraction correlates with the integrity of the blood-brain barrier, experiments are performed in which the blood-brain barrier is disrupted with a hyperosmolar solution of D-mannitol. Finally, images of the parameter used to calculate the extraction fraction are shown to be sensitive to mannitol, opening the possibility of MRI maps of extraction fraction without use of contrast agents.

THEORY

Figure 1 is a schematic representation of a typical fraction of tissue and its associated microvasculature. With the arterial spin-labeling technique, arterial water is selectively labeled proximal to the tissue. Blood flow brings this labeled water to the region of interest, where it can diffuse out of the vasculature and into the tissue to exchange with tissue water. According to this representation, it is considered that not all but only a CBF-dependent fraction, $E(f)$, of this labeled water is able to diffuse out of the vasculature and exchange with tissue water. $E(f)$ is called the "extraction fraction" for water. The remaining fraction, $1 - E(f)$, of the labeled water is unable to diffuse out of the vascular space and reaches the venous side of the vasculature without exchanging with tissue water. This model also considers magnetization transfer (MT) effects between tissue water and macromolecules.

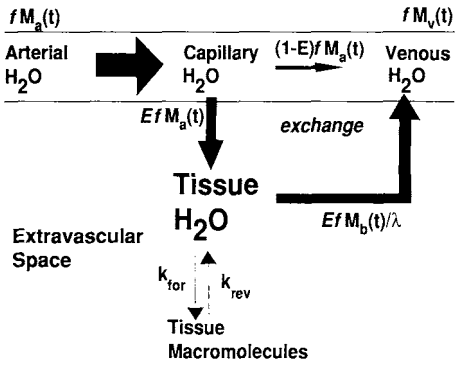

FIG. 1. Schematic representation of the modified model for measuring tissue perfusion. A unitary volume of tissue and its associated vasculature is shown. A blood-flow-rate-dependent fraction E(f) of labeled arterial water diffuses out of the vasculature and exchanges with tissue water. The other nondiffusable fraction 1 − E(f) of labeled arterial water reaches the venous side of the vasculature without exchanging with tissue water. Also included in this representation are the magnetization transfer (MT) effects caused by cross-relaxation between tissue water and tissue macromolecules.

According to this model, the Bloch equations for the longitudinal magnetization of brain tissue water and macromolecular spins per gram of tissue, which include T_1 relaxation, tissue perfusion, and magnetization transfer due to cross-relaxation, are given by:

$$\frac{dM_b(t)}{dt} = \frac{M_b^0 - M_b(t)}{T_{1b}} - k_{for}M_b(t) + k_{rev}M_m(t) + f[M_a(t) - M_v(t)] \quad [1a]$$

$$\frac{dM_m(t)}{dt} = \frac{M_m^0 - M_m(t)}{T_{1m}} + k_{for}M_b(t) - k_{rev}M_m(t) \quad [1b]$$

where:

f = tissue perfusion rate in ml · g^{-1} · s^{-1};

T_{1b}, T_{1m} = spin-lattice relaxation time constant of brain water proton spins and of macromolecular proton spins, respectively, in the absence of perfusion and cross-relaxation;

$M_b(t)$, $M_m(t)$ = longitudinal magnetization of tissue water protons and of macromolecular protons, respectively, per gram of brain tissue;

M_b^0, M_m^0 = equilibrium value of $M_b(t)$ and $M_m(t)$, respectively;

$M_a(t)$, $M_v(t)$ = longitudinal magnetization of water protons per ml of arterial blood and per ml of venous blood, respectively;

k_{for}, k_{rev} = magnetization transfer rate constants between tissue water protons and macromolecular protons, in s^{-1}.

When water can be considered as a freely diffusible tracer, the longitudinal magnetization of venous water can be written as:

$$M_v(t) = \frac{M_b(t)}{\lambda} \quad [2]$$

where λ is the brain-blood partition coefficient of water defined as (ml of water/g of brain tissue)/(ml of water/ml of blood). In the case of a diffusion-limited tracer, i.e., one that has extraction fraction $E < 1$, the arterial-venous concentration difference of the tracer is effectively reduced by the extraction fraction (Fig. 1), so that in Eq. [1a], $M_a(t) - M_v(t)$ should be substituted by $E(f)[M_a(t) - M_b(t)/\lambda]$. In other words, this substitution considers the extent to which blood water and tissue water equilibrate during the passage of blood water from the arterial side to the venous side of the microvasculature. Note that the

extraction fraction is written as a function of the perfusion rate.

Under equilibrium conditions, the amount of water flowing into the brain always equals the amount of water flowing out, so that:

$$f[M_a^0 - M_v^0] = fE(f)\left[M_a^0 - \frac{M_b^0}{\lambda}\right] = 0 \qquad [3]$$

When continuous adiabatic fast passage (24) is used to invert arterial water spins, one may write:

$$M_a(t) = (1 - 2\alpha)M_a^0 = (1 - 2\alpha)\frac{M_b^0}{\lambda} \qquad [4]$$

where α is the degree of arterial spin labeling, defined as $\alpha = \dfrac{M_a^0 - M_a(t)}{2M_a^0}$.

Under all conditions stated above, the resulting Bloch equations become:

$$\frac{dM_b(t)}{dt} = \frac{M_b^0 - M_b(t)}{T_{1b}} - k_{for}M_b(t) + k_{rev}M_m(t) - \frac{f}{\lambda}E(f)(2\alpha - 1)M_b^0 - \frac{f}{\lambda}E(f)M_b(t) \qquad [5a]$$

$$\frac{dM_m(t)}{dt} = \frac{\frac{k_{for}}{k_{rev}}M_b^0 - M_m(t)}{T_{1m}} + k_{for}M_b(t) - k_{rev}M_m(t) \qquad [5b]$$

Equations [5a] and [5b] can be solved for two different cases. In the first case, macromolecular spins are saturated by the RF irradiation used for arterial spin labeling, which is the typical situation when a single RF coil is used to label the arterial water spins and to detect the tissue water protons magnetization (3). In the second case, macromolecular spins are not disturbed by the RF irradiation used for arterial spin label. Both cases are discussed herein.

Case I: Brain Macromolecular Spins Saturated During Arterial Spin Labeling

When macromolecular spins are saturated ($M_m(t) = 0$ for all t), the solution of Eq. [5a] at the initial condition of $M_b(t) = 0) = M_b^0$ gives:

$$M_b(t) = T_{1app}M_b^0\left\{\frac{1}{T_{1app}} - \left[k_{for} + 2\alpha\frac{f}{\lambda}E(f)\right](1 - e^{-t/T_{1app}})\right\} \qquad [6]$$

with

$$\frac{1}{T_{1app}} = \frac{1}{T_{1b}} + k_{for} + \frac{f}{\lambda}E(f) \qquad [7]$$

At the steady state when RF is applied at a control plane (i.e., brain macromolecular spins are saturated without arterial spin labeling, $\alpha = 0$), Eq. [6] becomes:

$$M_b^{ss1} = T_{1app}\left[\frac{1}{T_{1b}} + \frac{f}{\lambda}E(f)\right]M_b^0 \qquad [8]$$

When RF is applied at a labeling plane (i.e., brain macromolecular spins are saturated with arterial spin labeling), the steady state of Eq. [6] gives:

$$M_b^{ss2} = \left[1 - \frac{2\alpha\frac{f}{\lambda}E(f)}{\frac{1}{T_{1b}} + \frac{f}{\lambda}E(f)}\right]M_b^{ss1} \qquad [9]$$

Using Eqs. [7]–[9], the brain tissue relaxation time T_{1b}, the magnetization transfer rate constant k_{for} and the tissue perfusion rate f can be estimated from an appropriate measurement of T_{1app}, M_b^0, M_b^{ss1}, M_b^{ss2}, and α, according to:

$$T_{1b} = \frac{T_{1app}M_b^0}{M_b^{ss1}}\left[1 + \frac{M_b^{ss1} - M_b^{ss2}}{M_b^{ss2} + (2\alpha - 1)M_b^{ss1}}\right] \qquad [10]$$

$$k_{for} = \frac{1}{T_{1app}}\left(1 - \frac{M_b^{ss1}}{M_b^0}\right) \qquad [11]$$

and

$$f = \frac{\lambda}{E(f)}\frac{1}{T_{1b}}\left[\frac{M_b^{ss1} - M_b^{ss2}}{M_b^{ss2} + (2\alpha - 1)M_b^{ss1}}\right] \qquad [12]$$

The presence of the term $E(f)$ in the denominator of Eq. [12] indicates that the perfusion rate f is underestimated at large CBF if arterial water is assumed to be a freely diffusible perfusion tracer.

Case II: No Saturation of Brain Macromolecular Spins During Arterial Spin Labeling

Arterial spin labeling without saturation of brain macromolecular spins can be accomplished with a two-coil system (7). Tagging of the arterial water spins is accomplished by applying RF power to a labeling RF coil located in the neck region in the presence of a field gradient. When a good RF isolation between the labeling coil and the detection coil is obtained, the B_1 field generated by the labeling coil does not reach the detection volume in the brain, so that tagging of the arterial spins is accomplished without saturation of macromolecular spins in the region of interest (ROI) inside the brain.

The solution of Eq. [5] is then given by:

$$M_b(t) = M_b^{ss} + M_b^1 e^{-t/T_{1app1}} + M_b^2 e^{-t/T_{1app2}} \qquad [13a]$$

$$M_m(t) = M_m^{ss} + M_m^1 e^{-t/T_{1app1}} + M_m^2 e^{-t/T_{1app2}} \qquad [13b]$$

where M_b^{ss} and M_m^{ss} are the steady-state magnetization of tissue water and of macromolecular spins, respectively; M_b^1 and M_b^2 are the magnitudes of the two exponentially decaying components of the tissue water magnetization; M_m^1 and M_m^2 are the magnitudes of the two exponentially decaying components of the macromolecular magnetization; and:

$$\frac{1}{T_{1app1}} = \frac{1}{2}\left\{\frac{1}{T_{1app}} + \left(\frac{1}{T_{1m}} + k_{rev}\right)\right.$$

$$- \sqrt{\left[\left(\frac{1}{T_{1m}} + k_{rev}\right) - \frac{1}{T_{1pp}}\right]^2 + 4k_{for}k_{rev}}\Bigg\} \quad [14a]$$

$$\frac{1}{T_{1app2}} = \frac{1}{2}\Bigg\{\frac{1}{T_{1app}} + \left(\frac{1}{T_{1m}} + k_{rev}\right) + \sqrt{\left[\left(\frac{1}{T_{1m}} + k_{rev}\right) - \frac{1}{T_{1app}}\right]^2 + 4k_{for}k_{rev}}\Bigg\} \quad [14b]$$

are the two decay-rate constants of the coupled system.

The steady-state magnetization of tissue water, obtained with arterial spin labeling without saturation of brain macromolecular spins, is given by:

$$M_b^{ss} = \left[1 - \frac{2\alpha\frac{f}{\lambda}E(f)}{\frac{1}{T_{1b}} + \frac{f}{\lambda}E(f) + \delta}\right]M_b^0 \quad [15]$$

with

$$\delta = \frac{k_{for}}{1 + k_{rev}T_{1m}} \quad [16]$$

The perfusion rate f can be calculated from M_b^0 and M_b^{ss} according to:

$$f = \frac{\lambda}{E(f)}\left(\frac{1}{T_{1b}} + \delta\right)\frac{M_b^0 - M_b^{ss}}{M_b^{ss} + (2\alpha - 1)M_b^0} \quad [17]$$

From Eq. [17], it is clear that the perfusion rate f is underestimated at large CBF if the presence of the extraction fraction for water $E(f)$ in the denominator is neglected due to the assumption that arterial water is a freely diffusible tracer. It also can be seen that when macromolecular spins are not saturated, the quantitation of perfusion is affected by cross-relaxation between water and macromolecules, as indicated by the presence of the term δ. However, as shown in Eq. [16], δ is only dependent on the magnetization transfer rate constants, k_{for} and k_{rev}, and on the spin-lattice relaxation time constant of the macromolecular spins, T_{1m}. δ should, therefore, only depend on the B_0 field strength and on the tissue type but *not* on flow.

The value of δ can be determined experimentally in two different ways (8). The first way is by measuring k_{for}, k_{rev}, and T_{1m}. k_{for} can be obtained from brain water MT data according to Eq. [6] (with $\alpha = 0$ to determine T_{1app}) and Eq. [11], whereas k_{rev} and T_{1m} can be estimated from fit to brain water relaxation data without saturation of macromolecular spins using Eqs. [13a] and [14]. A value for δ, herein called $\delta_{relaxation}$, can then be calculated directly from k_{for}, k_{rev}, and T_{1m} according to Eq. [16]. The second way to evaluate δ is to measure perfusion both with and without saturation of macromolecular spins on the same subject under the same conditions. If the perfusion remains the same between the two measurements, Eqs. [12] and [17] can be combined so that this experimental value for δ, herein called $\delta_{perfusion}$, can be determined according to:

$$\delta_{perfusion} = \frac{1}{T_{1b}}\left[\frac{\frac{M_b^{ss1} - M_b^{ss2}}{M_b^{ss2} + (2\alpha - 1)M_b^{ss1}}}{\frac{M_b^0 - M_b^{ss}}{M_b^{ss} + (2\alpha - 1)M_b^0}} - 1\right] \quad [18]$$

It is interesting to notice that $\delta_{perfusion}$, as determined from Eq. [18], does not depend on the extraction fraction $E(f)$, as expected, nor does it depend on the blood flow rate f, provided that the signal intensities measured for M_b^0, M_b^{ss}, M_b^{ss1}, and M_b^{ss2} come from tissue water only and not from a mixture of tissue water and vascular water. To ensure that is the actual case, crusher gradients can be applied to the pulse sequence used in the measurement of perfusion to destroy any coherent magnetization coming from vascular (i.e., fast moving) spins.

If no crusher gradients are used, the presence of magnetization coming from water protons in the vascular bed must be taken into account. Considering a voxel of unitary volume as shown in Fig. 1, in which the vasculature occupies a fraction V of this volume and the tissue occupies a fraction $(1 - V)$, the NMR signal per unit volume obtained from this voxel is given by:

$$S = M_b(t)(1 - V)\rho_b + M_V(t)V \quad [19]$$

where ρ_b is the brain tissue density in g/cm^3 and $M_V(t)$ is the magnetization of water per milliliter of blood in the vasculature. This magnetization will have contributions from the fraction of arterial water that does not exchange with tissue water and from the water that diffuses out of the tissue back into the vasculature. Namely,

$$M_V(t) = [1 - E(f)]M_a(t) + E(f)\frac{M_b(t)}{\lambda} \quad [20]$$

The average tissue density can be related to the average brain-blood partition coefficient for water. In the particular case of the brain, assuming $\lambda = 0.9$ cm^3/g and $\rho_b = 1.1$ g/cm^3, the approximation $|\rho_b| \approx 1/|\lambda|$ can be used. This approximation only holds for water in the brain. For other tracers with different partition coefficients the relation between λ and ρ_b should be different. Therefore, using Eq. [4], Eq. [19] can be rewritten as:

$$S = \frac{M_b(t)}{\lambda}\{1 - [1 - E(f)]V\} + [1 - E(f)]V(1 - 2\alpha)\frac{M_b^0}{\lambda} \quad [21]$$

According to Eq. [21], when no crusher gradients are applied to destroy the magnetization coming from vascular spins, the signal intensity measured in the ROI has contributions from tissue water magnetization and also from vascular water magnetization. This equation can be used to calculate the signal intensity under the two experimental conditions outlined in cases I and II.

Case I: Brain Macromolecular Spins Saturated During Arterial Spin Labeling

a) Steady state when RF is applied at a control plane: In this case, $M_b(t) = M_b^{ss1}$ and $\alpha = 0$. Eq. [21] then reduces to:

$$S_{ss1} = \frac{M_b^{ss1}}{\lambda}\{1 - [1 - E(f)]V\} + [1 - E(f)]V\frac{M_b^0}{\lambda} \quad [22]$$

b) Steady state when RF is applied at a labeling plane: In this case, $M_b(t) = M_b^{ss2}$ and $\alpha \neq 0$. Eq. [21] then becomes:

$$S_{ss2} = \frac{M_b^{ss2}}{\lambda}\{1 - [1 - E(f)]V\} + 1 - E(f)]V(1 - 2\alpha)\frac{M_b^0}{\lambda} \quad [23]$$

Using Eqs. [9], [22], and [23], the blood flow rate f can be obtained as:

$$f = \frac{\lambda}{E(f)}\frac{1}{T_{1b}}\left[\frac{S_{ss1} - S_{ss2}}{S_{ss2} + (2\alpha - 1)S_{ss1}}\right] - \frac{2\alpha[1 - E(f)]V}{E(f)}\frac{1}{T_{1b}}\frac{M_b^0}{S_{ss2} + (2\alpha - 1)S_{ss1}} \quad [24]$$

The second term in Eq. [24] appears only if vascular spins are allowed to be observed in the NMR detection sequence used in the experiment, i.e., if they are not crushed and if water is not a freely diffusible tracer, i.e., if $E(f) < 1$. Note that this equation reduces exactly to Eq. [12] if the vasculature is crushed (equivalent to setting $V = 0$) or if water is a freely diffusible tracer (equivalent to making $E(f) = 1$).

Case II: No Saturation of Brain Macromolecular Spins During Arterial Spin Labeling

a) No RF power applied (equilibrium condition): In this case, $M_b(t) = M_b^0$ and $\alpha = 0$. Equation [21] then reduces to:

$$S_0 = \frac{M_b^0}{\lambda}\{1 - [1 - E(f)]V\} + [1 - E(f)]V\frac{M_b^0}{\lambda} = \frac{M_b^0}{\lambda} \quad [25]$$

b) Steady state when RF is applied at a labeling plane: In this case, $M_b(t) = M_b^{ss}$ and $\alpha \neq 0$. Eq. [21] then becomes:

$$S_{ss} = \frac{M_b^{ss}}{\lambda}\{1 - [1 - E(f)]V\} + [1 - E(f)]V(1 - 2\alpha)\frac{M_b^0}{\lambda} \quad [26]$$

Using Eqs. [15], [25], and [26], the blood flow rate f can be obtained as:

$$f = \frac{\lambda}{E(f)}\left(\frac{1}{T_{1b}} + \delta\right)\left[\frac{S_0 - S_{ss}}{S_{ss} + (2\alpha - 1)S_0}\right] - \frac{2\alpha[1 - E(f)]V}{E(f)}\left(\frac{1}{T_{1b}} + \delta\right)\frac{M_b^0}{S_{ss} + (2\alpha - 1)S_0} \quad [27]$$

Equations [24] and [27] can be combined to determine an experimental value for $\delta_{perfusion}$ when no crusher gradients are used in the experiment:

$$\delta_{perfusion} = \frac{1}{T_{1b}}\left[\frac{S_{ss1} - S_{ss2} - 2\alpha[1 - E(f)]V\frac{M_b^0}{\lambda}}{S_{ss2} + (2\alpha - 1)S_{ss1}} \Big/ \frac{S_0 - S_{ss} - 2\alpha[1 - E(f)]V\frac{M_b^0}{\lambda}}{S_{ss} + (2\alpha - 1)S_0} - 1\right] \quad [28]$$

Equation [28] shows how the expression for $\delta_{perfusion}$ is affected by the nonexchangeable labeled arterial water spins. The contribution of the vascular spins becomes more relevant at high CBF values, when the extraction fraction for water is significantly smaller than 1. Therefore, the error made by assuming that water is freely diffusible also increases with increasing CBF values. The value of the extraction fraction $E(f)$ can be calculated from Eq. [28] when a correct value for δ is inserted in the left side of that equation. For instance, if $\delta_{relaxation}$ as measured from the relaxation curves is used on the left hand side of Eq. [28], the extraction fraction $E(f)$ is given as:

$$E(f) = 1 - \frac{1}{2\alpha VS_0}\left[\frac{\frac{S_{ss1} - S_{ss2}}{S_{ss2} + (2\alpha - 1)S_{ss1}} - (T_{1b}\delta_{relaxation} + 1)\frac{S_0 - S_{ss}}{S_{ss} + (2\alpha - 1)S_0}}{\frac{1}{S_{ss2} + (2\alpha - 1)S_{ss1}} - (T_{1b}\delta_{relaxation} + 1)\frac{1}{S_{ss} + (2\alpha - 1)S_0}}\right] \quad [29]$$

Equation [29] shows how the extraction fraction for water can be measured from two perfusion experiments performed with and without saturation of tissue macromolecules.

MATERIALS AND METHODS

Animal and Surgical Methods

Male Sprague-Dawley rats (300–400 g, Taconic Farms, Germantown, NY) were anesthetized initially with 5% halothane. The rats were then intubated orally and kept on 2.5% halothane and a 1:1 N_2O/O_2 gas mixture using a rodent ventilator (Harvard Apparatus, South Natick, MA). The left femoral artery was cannulated with a PE-50 tube to monitor blood pressure and to sample arterial blood for gas analysis. The halothane level in the N_2O/O_2 gas mixture was reduced to 0.5% once the animal was placed in the magnet. A dose of 0.5 mg/200 g of pancuronium bromide (2 mg/ml in saline) (Organon Inc., West Orange, NJ) was administered initially to paralyze the rats and followed by a dose of 0.25 mg/200 g every 90 min intraperitoneally to maintain immobilization. Core body temperature was maintained with a heated water blanket.

CBF values were varied by adding CO_2 gas (0–10%) to the N_2O/O_2 gas mixture, and the P_aCO_2 and P_aO_2 were monitored periodically during the experiments with a blood gas analyzer machine (ABL Systems). In the experiments to disrupt the blood-brain barrier, a PE-50 tube was inserted in the left femoral vein before the animal was placed in the magnet. A dose of 5 ml/kg of a 25% solution of D-mannitol was infused into the femoral vein at a rate of about 0.11 ml/s.

NMR Methods

NMR experiments were performed on a 4.7 T, 40-cm-bore Bruker BIOSPEC II spectrometer equipped with a 15-cm

gradient insert. A two-coil system, consisting of a 0.5-cm-diameter butterfly-shaped labeling RF coil and a 3-cm-diameter saddle-shaped head coil as described in ref. 7, was used in all experiments. The two coils were decoupled actively by the action of PIN diodes to avoid saturation of macromolecular spins during the labeling period of the experiment. The isolation between the two coils was of the order of −74 dB (7).

A STEAM sequence (23) with $TE = 20$ ms and TM = 17 ms was used for volume-localized ($0.5 \times 0.5 \times 0.5$ cm^3) detection of brain tissue water magnetization. To avoid the influence of vascular moving spins in the experiment, crusher gradients of 4 G/cm, 4 ms duration, and 19 ms separation were applied in all three perpendicular directions inside the STEAM pulse sequence. Four scans were averaged for each measurement with a delay of 10 s between scans to allow for longitudinal relaxation.

Perfusion images were obtained by adding a 2-s labeling pulse before each phase-encoding step (TR = 2 s) on a spin-echo sequence with $TE = 30$ ms. The images were acquired using a coronal slice of the brain with a field of view of 5 cm, slice thickness of 2 mm, and matrix data size of 128×64, for a total acquisition time of 4 min 15 s.

Perfusion Measurements

Perfusion measurements using a volume-localized STEAM sequence were performed with and without saturation of brain macromolecular spins. For labeling the arterial spins by continuous adiabatic-fast-passage inversion (24), RF power was applied to the labeling coil with a B_1 intensity of about 100 mG at 0.5 cm above the center of the coil, which approximates the location of the carotid arteries. The RF power applied to the labeling coil was adjusted so that optimal arterial spin labeling was achieved. The degree of arterial spin labeling, $\alpha = 0.82$, was measured as described previously (7) and used for calculation of perfusion.

For perfusion measurements without saturation of tissue macromolecules, the two-coil system was operated with the labeling coil and the detection head coil was decoupled by the action of PIN diodes, so that when the labeling coil was tuned, the head coil was detuned and vice versa. The RF power applied to the labeling coil to invert the arterial spins was left on for 6 s at a labeling plane situated in the neck region with a frequency offset of 8500 Hz and in the presence of a longitudinal field gradient of 1 G/cm, before the measurement of the brain tissue water signal intensity M_b^{ss} as given by Eq. [15]. For measurement of the equilibrium signal intensity for brain tissue water, M_b^0, no RF power was applied to the labeling coil during that 6-s period.

For perfusion measurements with saturation of macromolecules, the two-coil system was used with the polarity of the voltage applied to the PIN diode of the labeling coil reversed so that both coils were tuned and coupled. Steady-state signal intensities for brain tissue water magnetization with arterial spin labeling (M_b^{ss2}) were measured by applying RF irradiation (8500 Hz frequency offset) through both the labeling coil and the detection coil so that macromolecular spins were saturated. In the control experiment, M_b^{ss1} was measured by switching the sign of the frequency offset to keep the macromolecules saturated without labeling of the arterial spins. In both cases, RF power was applied in the presence of a longitudinal field gradient of 1 G/cm during a 3.5-s period before the STEAM acquisition of the brain tissue water signal intensity. A shorter relaxation delay was used here because the apparent relaxation time of tissue water (T_{1app}) is reduced when tissue macromolecular spins are saturated due to magnetization transfer (MT) effects (3).

Magnetization Transfer Relaxation Curve

This experiment consisted of applying RF power (100 mG) with a frequency offset of 8500 Hz to the detection coil during a saturation time T_s, which varied from 0 to 2 s in 0.1-s intervals, to cause saturation of brain macromolecules as previously described (3). Tissue water magnetization was sampled after the RF irradiation, as shown in Fig. 2A. Twenty STEAM-localized free induction decays (FIDs) with incremented T_s were acquired and the data were fitted to Eq. [6] (with $\alpha = 0$) to determine values of M_b^0, M_b^{ss1}, and T_{1app}. The magnetization transfer rate constant k_{for} was also determined according to Eq. [11].

Relaxation Curve Without Saturation of Brain Macromolecular Spins

A normal inversion-recovery sequence without saturation of macromolecular spins and with the time delay (TI) after the inversion pulse varying from 0 to 6 s before the STEAM acquisition was used to measure relaxation curves as described previously (8) (Fig. 3B). Spin inversion was achieved by applying an on-resonance 180° RF pulse, which had a typical duration of 300 μs. Twenty data points were acquired and fitted to Eq. [13a] to obtain the long apparent spin-lattice relaxation time constant T_{1app1} and the short apparent spin-lattice relaxation time constant T_{1app2}. To make the estimate of T_{1app2} more reliable, many points were taken at short TI (10 points from 0 to 100 ms). From the determined values for T_{1app1} and T_{1app2}, the magnetization transfer rate constant k_{rev} and the spin-lattice relaxation time constant of brain macromolecular proton spins T_{1m} were calculated from Eq. [14].

δ Measurements

Four different experiments were performed to measure δ as given by Eq. [16]:

(a) $\delta_{relaxation}$: In the first experiment, values for k_{for}, k_{rev}, and T_{1m} were estimated from the relaxation curves obtained with and without saturation of brain macromolecules from 25 rats at various CBF values and used to produce a value for $\delta_{relaxation}$.

(b) $\delta_{perfusion}$: In the second experiment, perfusion measurements with and without saturation of brain macromolecules were performed sequentially in nine rats at various CBF values using a volume-localized STEAM sequence with crusher gradients applied to remove the contribution from vascular spins. Assuming that the perfusion remained the same between the two measure-

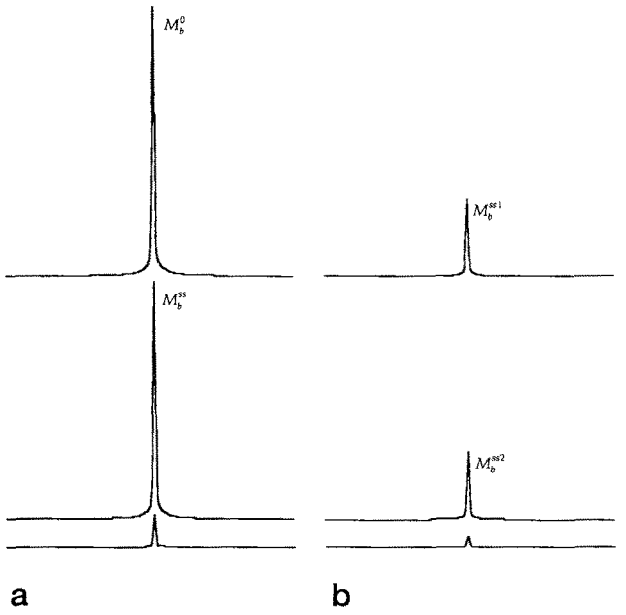

FIG. 2. (A) A typical set of spectra obtained when the two-coil system was used for STEAM-localized measurement of perfusion. Scale is normalized to the peak value of the spectrum representing M_b^0 (top left), which was obtained when macromolecules were not saturated. The spectrum representing M_b^{ss} (center left) was obtained when RF power was applied to the labeling coil at the labeling plane. The difference spectrum is shown in the bottom left. (B) Spectra obtained from the same rat when macromolecules were saturated. Scale is the same as (A), to show decrease in signal intensity caused by MT effects. M_b^{ss1} (top right) was obtained by applying RF at the control frequency, whereas M_b^{ss2} (center right) was obtained when the RF power was selective at the labeling frequency, causing saturation of macromolecules and arterial spin labeling. The difference spectrum is shown at the bottom right.

ments, a value for $\delta_{perfusion}$ was determined according to Eq. [18].

(c) $\delta_{perfusion}$ *with vascular spins:* In the third experiment, the crusher gradients used in the STEAM sequence were removed to allow observation of vascular spins. Perfusion measurements with and without saturation of brain macromolecules were performed in 38 rats at varying CBF values to allow the measurement of $\delta_{perfusion}$ when vascular water spins are also detected together with tissue water.

(d) $\delta_{perfusion}$ *with mannitol:* In the fourth experiment, the STEAM sequence was used without crusher gradients to access the value of $\delta_{perfusion}$ after breaking the blood-brain barrier with an intravenous injection of a solution of D-mannitol as described previously in the Animal and Surgical Methods section. This experiment was performed in seven rats at high CBF rates (>2.5 ml/g min).

δ Images

Perfusion images with and without saturation of brain macromolecules were taken using a spin-echo sequence. No crusher gradients were added to the imaging sequence, and δ images were formed from the perfusion images according to Eq. [18]. These images were obtained before and after breaking the blood-brain barrier with an intravenous injection of D-mannitol as described in the Animal and Surgical Methods section.

RESULTS

Figure 2 shows a typical set of four spectra from the perfusion measurement of a rat brain under normocarbic conditions (pCO_2 = 38.5 mmHg). Fig. 2A shows two spectra acquired for a rat brain with the volume localized STEAM sequence with the two-coil system in the decoupled mode, corresponding to the brain tissue water signal intensity under equilibrium conditions (M_b^0, top spectrum) and with labeling of the arterial spins (M_b^{ss}, center spectrum). The vertical scale was normalized to the peak value of the spectrum representing M_b^0 (top spectrum). In this particular case, the center spectrum representing M_b^{ss} has a peak value of 0.90. The bottom spectrum corresponds to the difference between the top spectrum (M_b^0) and the center spectrum (M_b^{ss}) and is proportional to the perfusion rate f according to Eq. [17].

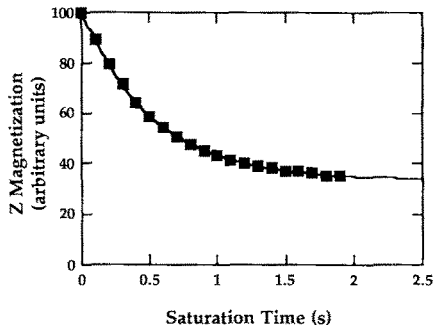

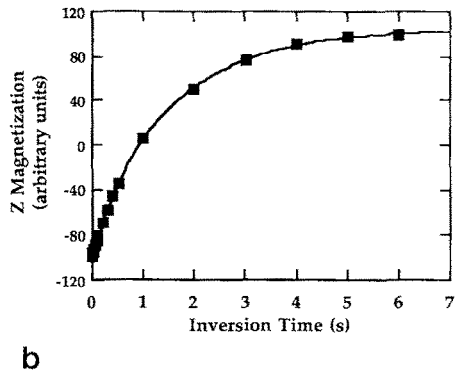

FIG. 3. (A) Magnetization transfer curve representing the change in brain water signal intensity when macromolecules are saturated without labeling of arterial spins. The horizontal axis represents the saturation time during which RF is applied. In this case, fitting of the data to a monoexponential curve gives T_{1app} = 0.52 ± 0.01 s and M_b^{ss1}/M_b^0 = 0.335 ± 0.003 (R = 0.99978). (B) Inversion-recovery experiment, for the same rat as in Fig. 2, during which macromolecules were not saturated and no arterial spin labeling occurs. Fitting of these data to Eq. [13a] gives T_{1app1} = 1.36 s and T_{1app2} = 0.03 s (R = 0.99998).

Figure 2B shows two spectra acquired with the STEAM sequence for the same rat as in Fig. 2A with the two-coil system in the coupled mode, corresponding to the brain tissue water signal intensity when brain macromolecules are saturated without (M_b^{ss1}, top spectrum) and with labeling of the arterial spins (M_b^{ss2}, center spectrum). The difference spectrum is shown on the bottom and is proportional to the perfusion rate f according to Eq. [12]. The vertical scale was kept the same as in Fig. 2A to show the decrease in tissue water signal intensity that occurs due to MT effects when tissue macromolecules are saturated (compare $M_b^{ss1} = 0.29$ to $M_b^0 = 1$). The decrease in signal intensity when macromolecules were saturated is evident, consequently resulting in a smaller signal-to-noise ratio when macromolecular spins were saturated as compared to when macromolecular spins were not saturated.

Figure 3A shows a typical MT data set obtained with the volume-localized STEAM sequence for the measurement of T_{1app}. The data shown in Fig. 3A were fitted to a monoexponential decay corresponding to Eq. [6] (with α set to 0) and represents the MT curve from tissue water to macromolecules when macromolecular spins are saturated. For this particular case, data fitting produced $T_{1app} = 0.52 \pm 0.01$ s and $M_b^{ss1}/M_b^0 = 0.335 \pm 0.003$ ($R = 0.99978$). $T_{1b} = 1.74 \pm 0.05$ s and $k_{for} = 1.28 \pm 0.03\ s^{-1}$ were calculated from the data shown in Fig. 3A using Eqs. [10] and [11], in agreement with previously reported values (3).

Figure 3B shows a typical inversion-recovery relaxation data curve obtained without saturation of macromolecular spins used to determine T_{1app1} and T_{1app2} from the same rat as for Fig. 3A. $T_{1app1} = 1.40 \pm 0.04$ s and $T_{1app2} = 0.04 \pm 0.03$ s ($R = 0.99998$) were obtained by fitting these data to Eq. [13a]. From Eq. [14], the MT rate constant k_{rev} was estimated to $k_{rev} = 23.99\ s^{-1}$ and the macromolecular spin-lattice relaxation time constant T_{1m} was estimated to $T_{1m} = 0.49$ s. By inserting the values of k_{for}, k_{rev}, and T_{1m} into Eq. [16], a value of $\delta_{relaxation} = 0.10\ s^{-1}$ was obtained. Table 1 summarizes the values of T_{1app}, T_{1app1}, T_{1app2}, T_{1b}, T_{1m}, k_{for}, k_{rev}, and $\delta_{relaxation}$ measured in 25 rats at varying CBF rates from the relaxation data.

Perfusion measurements with and without saturation of macromolecules were performed sequentially using the volume-localized STEAM sequence. Assuming that the perfusion rate f remained the same between the two experiments, values for $\delta_{perfusion}$ were determined from M_b^0, M_b^{ss}, M_b^{ss1}, M_b^{ss2}, and a value for T_{1b} of 1.65 s (Table 1) according to Eq. [18]. This experiment was performed under two different conditions. In the first case, crusher gradients were applied to the STEAM sequence to destroy any coherent magnetization coming from fast-moving spins. This condition was performed on nine rats at CBF rates that varied from 1.1 ml/g/min to 3.7 ml/g/min. The mean value for $\delta_{perfusion}$ in this case was $\delta_{perfusion} = 0.08 \pm 0.09\ s^{-1}$, in agreement with the mean value for $\delta_{relaxation}$ obtained from the relaxation data curves reported in Table 1, $\delta = 0.08 \pm 0.06\ s^{-1}$.

In the second case, the crusher gradients were removed from the STEAM sequence so that vascular water spins could be observed together with tissue water spins. This condition was applied to 38 rats with CBF rates that varied from 1.20 ml/g/min to 5.52 ml/g/min. Results of this experiment are plotted in Fig. 4, which shows the variation of $\delta_{perfusion}$, as calculated according to Eq. [18], with the CBF rate. Animals within 0.5 ml/g/min perfusion were combined leading to the x axis error bars. Figure 4 also shows the variation of $\delta_{relaxation}$ with the CBF rate. It can be seen that when no crushers are applied to the STEAM sequence, the values of $\delta_{relaxation}$ and $\delta_{perfusion}$ agree quite well for normal CBF rates (up to 1.5 ml/g/min). Above this flow rate value, $\delta_{perfusion}$ shows an increase with increasing flow rates, whereas $\delta_{relaxation}$ remains constant at values close to $0.1\ s^{-1}$. This difference becomes significant at blood flows greater than 3 ml/g/min ($P < 0.002$).

Table 2 summarizes the measurement of δ at high CBF values under the four different experimental conditions outlined in the Materials and Methods section. It can be seen in Table 2 that even at high flow rates, the measurement of $\delta_{perfusion}$ with crusher gradients present in the STEAM sequence agrees quite well with $\delta_{relaxation}$ (compare the first row to the second row in Table 2). But when the crusher gradients are removed from the detection sequence so that vascular spins can be observed, the value of $\delta_{perfusion}$ becomes very high (Table 2, third row). When the blood-brain barrier is damaged with a hyperosmolar solution of D-mannitol (Table 2, fourth row), the value of $\delta_{perfusion}$ at high flow decreases significantly ($P < 0.05$).

The extraction fraction for water can be calculated according to Eq. [29] from the experiment in which no crusher gradients are applied and the experiment to measure $\delta_{relaxation}$. A constant CBV of 5% was assumed throughout this study (25), although it is well known that increased $PaCO_2$ causes vasodilation (26, 27). Fig. 5 shows a plot of the extraction fraction as a function of CBF for the same rats used in the measurement of $\delta_{perfusion}$ shown in Fig. 4. It can be seen that the extraction fraction drops from about 1 for CBF values up to 1.0 ml/g/min to about 0.46 for CBF values around 5.2 ml/g/min.

Figure 6 shows a set of coronal perfusion images of a rat brain under hypercarbic conditions obtained without (Fig. 6A) and with (Fig. 6B) saturation of brain macromolecules before (left) and after (right) breaking the blood-brain barrier with an intravenous dose of 5 ml/kg of a solution of 25% mannitol. Fig. 6C shows the corre-

Table 1
Parameters Determined from the Relaxation Data as Illustrated in Figs. 3A and 3B ($n = 25$)

Parameter	T_{1app} (s)	T_{1app1} (s)	T_{1app2} (s)	T_{1b} (s)	T_{1m} (s)	k_{for} (1/s)	k_{rev} (1/s)	δ (1/s)
Mean	0.52	1.47	0.04	1.65	1.13	1.27	33.88	0.08
Standard Dev.	0.06	0.08	0.03	0.21	0.94	0.21	29.16	0.06

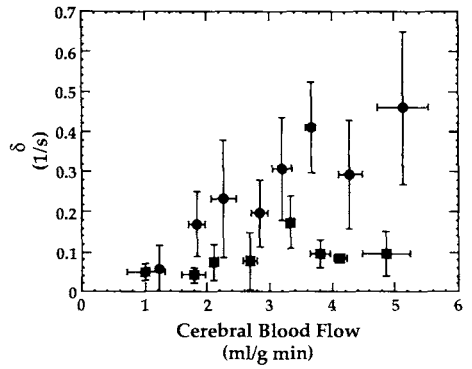

FIG. 4. Plot of $\delta_{perfusion}$ (circles) as measured without crusher gradients applied to the STEAM sequence and δ (squares) as a function of CBF. δ remains fairly constant at around 0.08 s^{-1}, but $\delta_{perfusion}$ increases dramatically with increasing CBF values due to the increasing contribution of nonexchangeable labeled vascular spins. Error bars = 1 SD.

sponding $\delta_{perfusion}$ images obtained according to Eq. [18]. The decrease in signal intensity in the image on the right is very clear and indicates that damage to the blood-brain barrier is highly correlated with changes in the value of the $\delta_{perfusion}$. In the case shown, there was a 35% decrease in $\delta_{perfusion}$ averaged over the entire slice. These results indicate that a $\delta_{perfusion}$ image can be calculated from perfusion images with and without MT effects.

DISCUSSION

A major issue associated with the application of techniques that rely on arterial water as a perfusion tracer to the brain is the validity of the freely diffusible tracer assumption for water. Considerable evidence presented in the literature (18–22) has contested this assumption and pointed out that the blood-brain barrier is a major limitation for exchange of blood water with tissue water. Reduced extraction fractions for water have been reported in the rat brain (19) and in the rhesus monkey and baboon brain (18, 20–22). This study attempts to estimate the extraction fraction for water in the rat brain with NMR measurements of perfusion using arterial spin labeling.

In recent publications, the arterial spin labeling technique has been implemented in the rat brain using two different approaches: one that saturates brain macromolecules during the arterial spin tagging of blood water (1–6) and another that avoids saturation of tissue macromolecules by using a two-coil scheme for labeling arterial water and detecting brain water magnetization (7, 8). MT effects are heterogeneous. Blood experiences less MT effects than tissue. *In vitro* studies have shown that the MT ratio for stationary blood is on the order of 10% signal attenuation (28). At 4.7 T, using a stationary sample of artificial blood under the same conditions used for labeling arterial water (i.e., $B_1 \sim 100$ mG at 8500 Hz off-resonance), we found a maximum signal attenuation of 20% (unpublished data) due to MT effects. MT effects decrease with increasing blood flow velocities (28), and therefore, vascular water is expected to suffer very little MT effects in the rat brain when compared to tissue water. When labeling of arterial water is performed, inducing saturation of brain macromolecules, the amount of MT effects seen by this labeled water will depend on whether it has diffused out of the vasculature and exchanged with tissue water or whether it remains intravascular.

The parameter δ is sensitive to the amount of MT effects seen by labeled water due to the dependence on k_{for}, k_{rev}, and T_{1m}. The quantitation of δ can be performed according to two experiments; Fig. 4 summarizes the results of this quantitation. When $\delta_{relaxation}$ is calculated from estimates for k_{for}, k_{rev}, and T_{1m} obtained from the relaxation curves, no variation with blood flow is observed, because no arterial spin labeling is involved to differentiate vascular water from tissue water. However, when $\delta_{perfusion}$ is measured from a comparison of perfusion obtained with and without saturation of brain macromolecules, the arterial spin labeling imposes a differentiation of the tagged arterial water from the tissue water. When crusher gradients are used in the detection sequence to minimize the contribution from vascular spins, no flow dependence in the value of $\delta_{perfusion}$ is observed, as expected, because only labeled spins that exchanged with tissue water contribute to the signal. In addition, the value of $\delta_{perfusion}$ measured with crusher gradients is equal to $\delta_{relaxation}$. If no crusher gradients are employed, the amount of labeled water confined in the vasculature (which sees much less MT effects than the labeled water that exchanged with tissue water) increases with blood flow as the extraction fraction decreases. The corresponding effect on the measurement of $\delta_{perfusion}$ can be seen in Fig. 4. This variation of $\delta_{perfusion}$ with blood flow can be used to estimate the extraction fraction for water according to Eq. [29].

The measurement of the extraction fraction for water often relies on two independent measures of perfusion, one that uses water as the tracer and another that uses a freely diffusible tracer. In this paper, the two approaches for measuring perfusion with and without saturation of brain macromolecules are used to quantitate the extraction fraction for water in the rat brain at various CBF values. Because both approaches use endogenous arterial water as a perfusion tracer, the measurement of the extraction fraction for water can be performed in a completely noninvasive manner.

Figure 5 shows the extraction fraction for water as measured using the arterial spin-labeling technique in the rat brain. At a CBF of 5.13 ± 0.40 ml/g/min, the extraction fraction measured was 0.46 ± 0.17. Gwan Go *et al.* found a smaller value of 0.32 ± 0.04 using an intracarotid bolus injection of radioactive-labeled water (19). It should be noticed from Eq. [29] that the value of the extraction fraction depends on the value of the cerebral blood volume (CBV). In this work, a blood-flow-independent value of $V = 5\%$ was assumed for the CBV in the rat brain (25). Gwan Go *et al.* assumed a value of 3% (19). If we had assumed the same CBV of 3% in this study, we would have obtained a value of 0.35 ± 0.12 for the extraction fraction at a CBF of 5.13 ± 0.40 ml/g/min, which is in better agreement to the value reported by Gwan Go *et al.* It is known that changes in $PaCO_2$ induces vasodilation (26, 27), so that CBV is likely to increase

Table 2
Measurement of δ at High CBF Rates According to Four Different Experiments

Experiment	*n*	Cerebral blood flow rate (ml/g min)	δ (1/s)
Relaxation data	9	4.00 ± 0.58	0.11 ± 0.05
Crusher gradients	9	2.82 ± 0.77	0.08 ± 0.09
No crusher gradients	9	4.34 ± 0.68	0.42 ± 0.12
D-mannitol	7	3.74 ± 1.12	0.29 ± 0.11

The last two rows show how the disruption of the blood-brain barrier affects the measure of δ when no crusher gradients are used in the detection sequence. The decrease in the value of δ after the injection of D-mannitol is statistically significant ($P < 0.05$).

with increased CBF. Admittedly, a better estimation of the CBV as a function of CBF should provide a more accurate measure for the extraction fraction. However, the data shown in Fig. 5 clearly represent evidence of the diffusion limitation of water in the brain at elevated blood flow.

Another point of concern in this study is the use of a volume-localized sequence to measure water signal intensity in the brain. The slice-selective gradients used by the STEAM sequence to localize a 125 μl volume in the brain are likely to attenuate some of the vascular water spins, even when no crushers are applied. This would cause an overestimation of the extraction fraction. It also is not clear whether the crushers were able to completely suppress vascular spins, but the excellent agreement between $\delta_{perfusion}$ as measured with crushers and $\delta_{relaxation}$ at all blood flows is good evidence that the crusher gradients were effective in removing the vascular spin contribution. In addition to a correct value for the cerebral blood volume, some other possible explanations can be found for the difference between our results and those published by Gwan Go *et al.* (19). Bolus tracer injections assume that the bolus of injected tracer can be represented as a Δ function that labels the tissue uniformly at time $t = 0$ and that no further tracer enters the tissue at times $t > 0$ (29). Also, the tracer's distribution volume must be large compared to the vascular volume of the tissue. Any deviations from this case may lead to an underestimation of the extraction fraction. Another possible explanation is that the model used here neglects longitudinal relaxation of the labeled water in the vasculature. If the loss of label of this nonexchangeable water due to relaxation before the measurement of the signal is significant, an overestimation of the extraction fraction occurs. This is because any relaxation of labeled water in the vasculature minimizes the vascular contribution in the perfusion experiment.

Due to its ability to detect changes in the extraction fraction for water, the arterial spin-labeling technique can be used to detect problems associated with the integrity of the blood-brain barrier. The $\delta_{perfusion}$ images shown in Fig. 6 are a clear indication that damage to the blood-brain barrier can be detected *noninvasively* using this technique. It should be noticed, however, that changes in water permeability in the brain are easier to detect at high flow rates than at low flow rates, at which changes in the extraction fraction for water are larger.

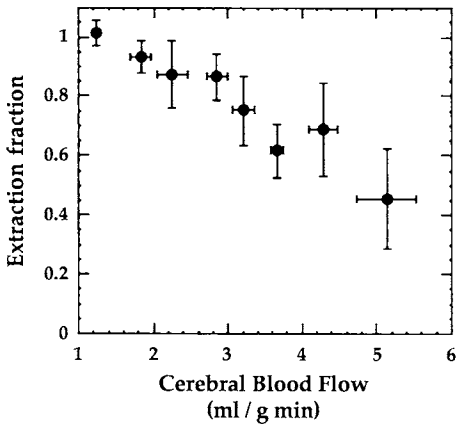

FIG. 5. Plot of the extraction fraction for water as a function of CBF in rat brain. The decrease in the value of the extraction fraction with increasing CBF is very clear, showing that water cannot be considered as a freely diffusable tracer in the rat brain at CBF values higher than 2 ml/g/min. Error bars = 1 SD.

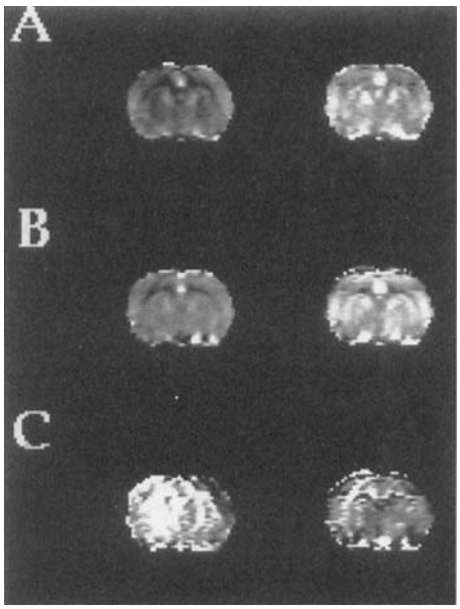

FIG. 6. (A) Coronal perfusion image of a rat brain measured without saturation of brain macromolecules using the two-coil system in the decoupled mode, before (left) and after (right) breaking the blood-brain barrier with an intravenous dose of 5 ml/kg of a solution of 25% mannitol. (B) Coronal perfusion image of a rat brain measured with saturation of brain macromolecules using the two-coil system in the coupled mode, before (left) and after (right) breaking the blood-brain barrier with the mannitol solution. (C) Corresponding $\delta_{perfusion}$ images obtained before (left) and after (right) breaking the blood-brain barrier with the mannitol solution. Notice the decrease in signal intensity in the image on the right, showing the ability to detect noninvasively the integrity of the blood-brain barrier.

A major shortcoming of the approach used here to assess the extraction fraction for water is that a difference of small differences must be detected, as shown by Eq. [29]. For example, in the rat brain, these differences are on the order of up to 13%. Whereas these changes can be measured in the rat brain at elevated flows, it will be challenging to detect the smaller changes expected in humans. The ability to assess extraction by comparing perfusion with and without MT effects is not limited to steady-state arterial spin labeling. The approach used here can be applicable to other techniques that use endogenous water to measure perfusion (13–17).

In conclusion, the theory has been developed and experiments have been conducted to examine the effects of the extraction fraction for water in the measurement of perfusion with the arterial spin-labeling technique. It is shown that the extraction fraction can be estimated noninvasively and should be accounted for in the measurement of rat brain perfusion at elevated blood flows. The ability to detect changes in the value of the extraction fraction makes the arterial spin-labeling technique capable of assessing the integrity of the blood-brain barrier.

ACKNOWLEDGMENTS

The authors thank Donald Bennett, Maryann Butowitz, and Cândida C. Silva for their technical assistance.

REFERENCES

1. J. A. Detre, J. S. Leigh, D. S. Williams, A. P. Koretsky, Perfusion imaging. *Magn. Reson. Med.* **23,** 37–45 (1992).
2. D. S. Williams, J. A. Detre, J. S. Leigh, A. P. Koretsky, Magnetic resonance imaging of perfusion using spin inversion of arterial water. *Proc. Natl. Acad. Sci. USA* **89,** 212–216 (1992).
3. W. Zhang, D. S. Williams, J. A. Detre, A. P. Koretsky, Measurement of brain perfusion by volume-localized NMR spectroscopy using inversion of arterial water spins: accounting for transit time and cross-relaxation. *Magn. Reson. Med.* **25,** 362–371 (1992).
4. D. S. Williams, J. A. Detre, W. Zhang, A. P. Koretsky, Fast serial MRI of perfusion in the rat brain using spin inversion of arterial water. *Bull. Magn. Reson.* **15,** 60–63 (1993).
5. W. Zhang, D. S. Williams, A. P. Koretsky, Measurement of rat brain perfusion by NMR using spin labeling of arterial water: *in vivo* determination of the degree of spin labeling. *Magn. Reson. Med.* **29,** 416–421 (1993).
6. E. G. Walsh, K. Minematsu, J. Leppo, S. C. Moore, Radioactive microsphere validation of a volume localized continuous saturation perfusion measurement. *Magn. Reson. Med.* **31,** 147–153 (1994).
7. A. C. Silva, W. Zhang, D. S. Williams, A. P. Koretsky, Multi-slice MRI of rat brain perfusion during amphetamine stimulation using arterial spin labeling. *Magn. Reson. Med.* **33,** 209–214 (1995).
8. W. Zhang, A. C. Silva, D. S. Williams, A. P. Koretsky, NMR measurement of perfusion using arterial spin labeling without saturation of macromolecular spins. *Magn. Reson. Med.* **33,** 370–376 (1995).
9. D. S. Williams, W. Zhang, A. P. Koretsky, S. Adler, Perfusion imaging of the rat kidney with MR. *Radiology* **190,** 339–344 (1994).
10. D. S. Williams, D. J. Grandis, W. Zhang, A. P. Koretsky, Magnetic resonance imaging of perfusion in the isolated rat heart using inversion of arterial water. *Magn. Reson. Med.* **30,** 361–365 (1993).
11. D. A. Roberts, J. A. Detre, L. Bolinger, E. K. Insko, J. S. Leigh, Jr., Quantitative magnetic resonance imaging of human brain perfusion at 1.5 T using steady-state inversion of arterial water. *Proc. Natl. Acad. Sci. USA* **91,** 33–37 (1994).
12. J. A. Detre, W. Zhang, D. A. Roberts, A. C. Silva, D. S. Williams, D. J. Grandis, A. P. Koretsky, J. S. Leigh, Jr., Tissue specific perfusion imaging using arterial spin labeling. *NMR Biomed.* **7,** 75–82 (1994).
13. R. R. Edelman, B. Siewert, D. G. Darby, V. Thangaraj, A. C. Nobre, M. M. Mesulam, S. Warach, Quantitative mapping of cerebral blood flow and functional localization with echo-planar MR imaging and signal targeting with alternating radio frequency. *Radiology* **192,** 413–520 (1994).
14. K. K. Kwong, J. W. Belliveau, D. A. Chesler, I. E. Goldberg, R. M. Weisskoff, B. P. Poncelet, D. N. Kennedy, B. E. Hopel, M. S. Cohen, R. Turner, H.-M. Cheng, T. J. Brady, B. R. Rosen, Dynamic magnetic resonance imaging of human brain activity during primary sensory stimulation. *Proc. Natl. Acad. Sci. USA* **89,** 5675–5679 (1992).
15. K. K. Kwong, D. A. Chesler, R. M. Weisskoff, K. M. Donahue, T. L. Davis, L. Ostergaard, T. A. Campbell, B. R. Rosen, MR perfusion studies with T1 weighted echo planar imaging. *Magn. Reson. Med.* **34,** 878–887 (1995).
16. S.-G. Kim, Quantitative of relative cerebral blood flow change by flow-sensitive alternating inversion recovery (FAIR) technique: application to functional MR imaging. *Magn. Reson. Med.* **34,** 293–301 (1995).
17. C. Schwarzbauer, S. P. Morrissey, A. Haase, Quantitative magnetic resonance imaging of perfusion using magnetic labeling of water proton spins within the detection slice. *Magn. Reson. Med.* **35,** 540–546 (1996).
18. J. O. Eichling, M. E. Raichle, R. L. Grubb, Jr., M. M. Ter-Pogossian, Evidence of the limitations of water as a freely diffusible tracer in the brain of the rhesus monkey. *Circ. Res.* **35,** 358–364 (1974).
19. K. Gwan Go, A. A. Lammertsma, A. M. J. Paans, W. Vaalburg, M. G. Woldring, Extraction of water labeled with oxygen 15 during single-capillary transit. *Arch. Neurol.* **38,** 581–584 (1981).
20. M. E. Raichle, R. W. Martin, P. Herscovitch, M. A. Mintum, J. Markham, Brain blood flow measured with intravenous $H_2{}^{15}O$. II. Implementation and validation. *J. Nucl. Med.* **24,** 790–798 (1983).
21. P. Herscovitch, M. E. Raichle, M. R. Kilbourn, M. J. Welch, Positron emission tomographic measurement of cerebral blood flow and permeability-surface area product of water using [^{15}O] water and [^{11}C] butanol. *J. Cereb. Blood Flow Metab.* **7,** 527–542 (1987).
22. K. B. Larson, J. Markham, M. E. Raichle, Tracer-kinetic models for measuring cerebral blood flow using externally detected radiotracers. *J. Cereb. Blood Flow Metab.* **7,** 443–463 (1987).
23. J. Frahm, K. D. Merboldt, W. Hanick, Localized proton spectroscopy using stimulated echoes. *J. Magn. Reson.* **72,** 502–508 (1987).
24. W. T. Dixon, L. N. Du, D. D. Faul, M. Gado, S. Rossnick, Projection angiograms of blood labeled by adiabatic fast passage. *Magn. Reson. Med.* **3,** 454–462 (1986).
25. P. Sandor, J. Cox-van Put, W. de Jong, D. de Wied, Continuous measurement of cerebral blood volume in rats with the photoelectric technique: effect of morphine and naloxone. *Life Sci.* **39(18),** 1657–1665 (1986).
26. R. L. Grubb, Jr., M. E. Raichle, J. O. Eichling, M. M. Ter-Pogossian, The effects of changes in $PaCO_2$ on cerebral blood volume, blood flow, and vascular mean transit time. *Stroke* **5(5),** 630–639 (1974).
27. J. O. Eichling, M. E. Raichle, R. L. Grubb, Jr., K. B. Larson, M. M. Ter-Pogossian, In vivo determination of cerebral blood volume with radioactive oxygen-15 in the monkey. Circ. Res. **37,** 707–711 (1975).
28. V. Dousset, P. Degrèze, S. Mièze, M. Sesay, B. Basse-Cathalinat, J.-M. Caillé, Magnetization transfer on in vitro circulating blood: implications for time-of-flight MR angiography. *J. Magn. Reson. Imaging* **5(6),** 786–788 (1995).
29. J. J. Neil, The use of freely diffusible, NMR-detectable tracers for measuring organ perfusion. *Concepts Magn. Reson.* **3,** 1–12 (1991).